

EVOLUTION OF THE OUT-OF-PLANE AMPLITUDE FOR QUASI-PERIODIC TRAJECTORIES IN THE EARTH-MOON SYSTEM

Thomas A. Pavlak*

Purdue University, United States of America
tpavlak@purdue.edu

Kathleen C. Howell†

Purdue University, United States of America
howell@purdue.edu

The out-of-plane amplitude along quasi-periodic trajectories in the Earth-Moon system is highly sensitive to perturbations in position and/or velocity as underscored recently by the ARTEMIS spacecraft. Controlling the evolution of the out-of-plane amplitude is non-trivial, but can be critical to satisfying mission requirements. The sensitivity of the out-of-plane amplitude evolution to perturbations due to lunar eccentricity, solar gravity, and solar radiation pressure is explored and a strategy for designing low-cost deterministic maneuvers to control the amplitude history is also examined. The method is sufficiently general and applied to the L_1 Lissajous orbit that serves as a baseline for the ARTEMIS P2 trajectory.

I. INTRODUCTION

For decades, the collinear libration points have been viewed as potentially useful locations to support both communications and scientific observations. Since the late 1970s, a number of missions have successfully operated in the vicinity of Sun-Earth collinear libration points including ISEE-3,¹ WIND,² SOHO,³ ACE,⁴ MAP,⁵ and Genesis.⁶ Despite the successes of past Sun-Earth libration point missions, no spacecraft had ever flown in the vicinity of an Earth-Moon libration point until August 2010 when the ARTEMIS P1 spacecraft entered an orbit near the Earth-Moon L_2 point. The ARTEMIS P2 probe became the second Earth-Moon libration point orbiter with an arrival near the L_2 point in October 2010. Due to the continuing success of the mission, it seems likely that interest in the Earth-Moon libration points will continue to increase.

The ARTEMIS libration point orbit design features Lissajous orbits with z -amplitudes, i.e., excursions normal to the lunar orbit plane, that vary greatly over the course of the mission. The evolution of the z -amplitude is highly sensitive to small perturbations in position or velocity. Deterministic correction maneuvers are designed and can deliver specific point solutions to ensure that the spacecraft trajectory retains the required lunar arrival conditions including inclination, several months into the future. However, these successfully designed corrections do not yield any

useful generalizations about the trajectory behavior at later epochs along the path or for future mission applications. Increasing the design intuition concerning the Lissajous trajectory evolution and the potential trade-off relationships in this dynamical environment is essential for effective future spacecraft operations in the Earth-Moon regime. It is desirable to understand the underlying dynamical structure that produces the z -amplitude evolution and to explore the sensitivity of this out-of-plane component to lunar eccentricity and solar perturbations. This analysis is accompanied by a comparison of results from numerical simulations in both the restricted three-body model and higher-fidelity Earth-Moon-Sun ephemeris models for the L_1 Lissajous trajectory that represents the path of the ARTEMIS P2 spacecraft. As will be demonstrated, initial studies indicate that lunar eccentricity, solar gravity, and solar radiation pressure create a small but non-negligible effect on z -amplitude evolution.

Numerical differential corrections algorithms are also required to both predict and control the evolution of these unstable trajectories via the determination of locations along the trajectory that are best-suited for deterministic maneuvers. This capability is explored by using some type of initial guess to compute a reference solution that likely does not satisfy specified constraints. Then, the path is decomposed into a series of segments and impulsive maneuvers are applied at various discrete locations along the trajectory. Ultimately, the process translates into a general search procedure to ensure that the spacecraft satisfies desired end-of-mission criteria at lunar orbit arrival despite the highly

*Ph.D. Student, School of Aeronautics and Astronautics

†Hsu Lo Professor of Aeronautical and Astronautical Engineering

sensitive Earth-Moon environment.

II. THE ARTEMIS MISSION

As the first libration point orbiter in the Earth-Moon system, the Acceleration Reconnection and Turbulence and Electrodynamics of the Moons Interaction with the Sun (ARTEMIS) mission represents a significant step in multi-body mission design and operations.⁷ ARTEMIS is an extension of the Time History of Events and Macroscale Interactions during Substorms (THEMIS) mission that was launched in 2007.⁸ The THEMIS mission originally consisted of five spacecraft in elliptical orbits about the Earth collecting measurements of the magnetosphere. A rendering of a THEMIS/ARTEMIS spacecraft appears in Fig. 1.

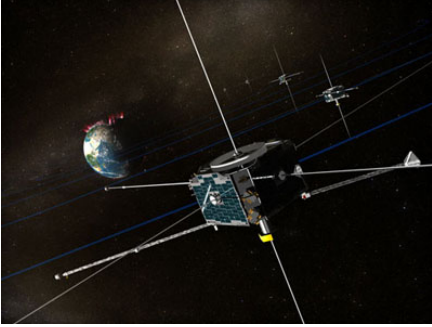


Fig. 1: THEMIS/ARTEMIS Rendering⁹

The ARTEMIS mission originated in July 2009, when two of the five THEMIS spacecraft, termed P1 and P2, initiated a series of orbit-raising maneuvers and lunar fly-bys to eventually depart the vicinity of the Earth. Closely following Sun-Earth and Earth-Moon manifolds, the P1 and P2 spacecraft each inserted into an orbit near the Earth-Moon L_2 libration point in August and October of 2011, respectively. The libration point orbiting phase of the ARTEMIS mission incorporates both L_1 and L_2 quasi-periodic Lissajous trajectories. Like most libration point orbits, the L_1 and L_2 Lissajous orbits, designed for the ARTEMIS spacecraft, are inherently unstable and sensitive to perturbations. Since both P1 and P2 spacecraft are operating only on propellant remaining from the THEMIS mission, efficient stationkeeping and orbit maintenance strategies are critical.^{10,11} While this analysis focuses on the ARTEMIS P2 orbit, the baseline trajectories for both spacecraft are presented for reference. Note that the information summarized in this investigation reflects the ARTEMIS baseline design as of August 2010.

II.I The ARTEMIS P1 Trajectory

The Earth-Moon libration point phase of the ARTEMIS P1 trajectory begins with insertion into an Earth-Moon L_2 Lissajous orbit on August 23, 2010. The P1 spacecraft orbits near the L_2 point for approximately 131 days before transferring to an L_1 Lissajous

orbit where it remains for an additional 85 days. After departing the L_1 vicinity, P1 is delivered into a retrograde lunar orbit such that periapsis occurs at an altitude of 1500 km on April 9, 2011. Three-dimensional and planar projections of the ARTEMIS P1 baseline trajectory appear in a Moon-centered rotating reference frames in Fig. 2(a) and 2(b), respectively. The final 1500 km \times 18,000 km (altitude) retrograde lunar orbit is included in red in Fig. 2(b).

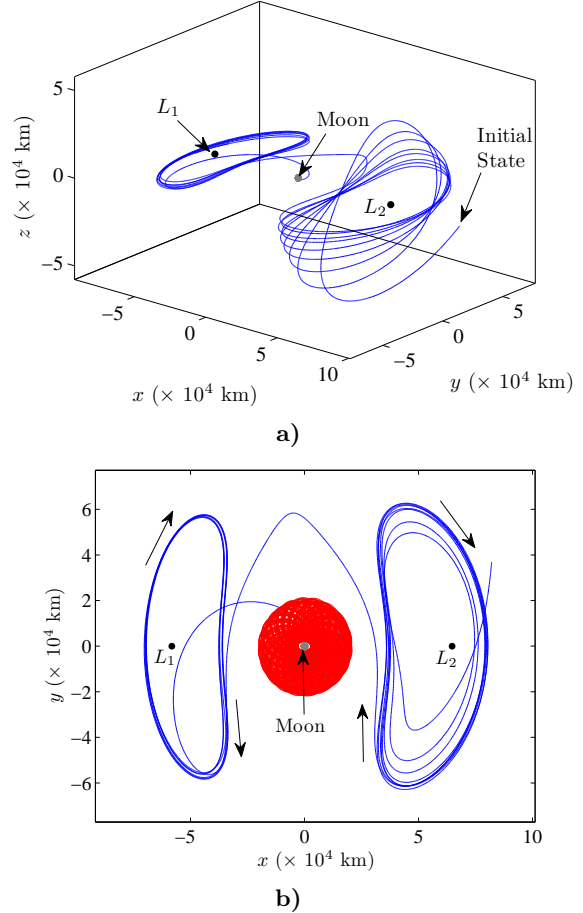


Fig. 2: ARTEMIS P1 Baseline Trajectory

II.II The ARTEMIS P2 Trajectory

The ARTEMIS P2 spacecraft arrives in the vicinity of the Earth-Moon L_2 libration point on October 3, 2010 and, rather than entering orbit near L_2 , the P2 spacecraft immediately shifts to a path that blends into an L_1 Lissajous orbit where it remains for approximately 154 days. The departure from the L_1 orbit delivers P2 to a prograde lunar arrival at a periapsis altitude of 1500 km. An isometric view of the ARTEMIS P2 baseline trajectory is plotted in Fig. 3(a) and a planar projection with the final 1500 km \times 18,000 km (altitude) orbit appears in Fig. 3(b).

III. SYSTEM MODELS

In this analysis, several dynamical models are employed to explore the effects of various perturbations

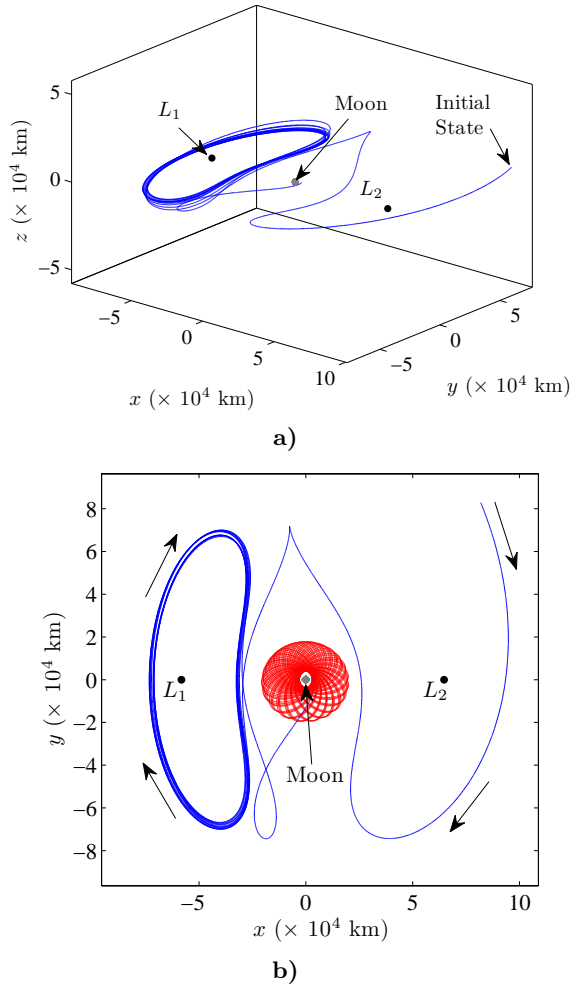


Fig. 3: ARTEMIS P2 Baseline Trajectory

on the z -amplitude evolution in a quasi-periodic Lissajous orbit and to demonstrate a strategy for placing deterministic maneuvers that correct an unfavorable z -amplitude evolution. The circular restricted three-body problem (CR3BP) serves as the framework for preliminary trajectory design activities and as the baseline dynamical model for the perturbation study. Employing the CR3BP is advantageous in preliminary analysis since the gravity of both the Earth and the Moon are incorporated simultaneously, but the time-invariant nature renders a formulation that offers significant advantages over higher-fidelity ephemeris models for initial analysis. An additional benefit of the CR3BP is that solutions obtained in this model can generally be transitioned to higher-fidelity models using straightforward differential corrections techniques.^{12,13}

III.I Restricted Three-Body Model

The circular restricted three-body problem is utilized to describe the motion of a body – in this case, a spacecraft – that is influenced by two gravity fields simultaneously, that is, the Earth and the Moon, under a set of simplifying assumptions. The spacecraft is

considered “massless” and the orbits of the Earth and Moon are modeled to be coplanar and circular relative to their barycenter. It is convenient to describe the CR3BP in terms of a rotating reference frame centered at the Earth-Moon barycenter in which the positive x -axis is oriented along the Earth-Moon line, the positive z -axis is parallel to the orbital angular momentum vector that reflects the orbits of the primaries, and the y -axis completes the right-handed triad. The masses of the two primaries are related through the nondimensional mass parameter, μ , defined as

$$\mu = \frac{m_M}{m_E + m_M} \quad [1]$$

where m_E is the mass of the Earth and m_M represents the mass of the Moon. The six-dimensional spacecraft state vector is denoted $\mathbf{x} = [x, y, z, \dot{x}, \dot{y}, \dot{z}]^T$, with bold symbols signifying vector quantities and position defined relative to the system barycenter. Then, the governing equations of motion in the CR3BP are written as nondimensional second-order scalar differential equations, i.e.,

$$\ddot{x} - 2\dot{y} - x = -\frac{(1-\mu)(x+\mu)}{d_1^3} - \frac{\mu(x-1+\mu)}{d_2^3} \quad [2]$$

$$\ddot{y} + 2\dot{x} - y = -\frac{(1-\mu)y}{d_1^3} - \frac{\mu y}{d_2^3} \quad [3]$$

$$\ddot{z} = -\frac{(1-\mu)z}{d_1^3} - \frac{\mu z}{d_2^3} \quad [4]$$

with the scalar relative distances,

$$d_1 = \sqrt{(x+\mu)^2 + y^2 + z^2} \quad [5]$$

$$d_2 = \sqrt{(x-1+\mu)^2 + y^2 + z^2} \quad [6]$$

such that d_1 and d_2 are measured from the Earth to the spacecraft and the Moon to the spacecraft, respectively. To compute trajectories in the CR3BP as well as higher-fidelity models, the vector equation of motion is expressed in first-order form as

$$\dot{\mathbf{x}} = \mathbf{f}(t, \mathbf{x}) \quad [7]$$

where position and velocity information are included in the six-dimensional state vector, \mathbf{x} .

III.II Higher-Fidelity Modeling

To explore the sensitivity of z -amplitude evolution in quasi-periodic orbits to various dynamical perturbations and to more accurately compute the magnitude and placement of deterministic ΔV maneuvers, higher-fidelity dynamical modeling is ultimately required. While the fidelity of the model is adjusted to assess the sensitivity of z -amplitude evolution to specific dynamical influences, the highest-fidelity model used in this analysis is a Moon-Earth-Sun point mass model incorporating the JPL DE405 ephemerides and

solar radiation pressure. Trajectories are computed in a Moon-centered, Earth J2000 reference frame using the equations of motion as expressed in second-order form, i.e.,

$$\ddot{\mathbf{r}}_{qi} = \mathbf{f}_g + \mathbf{f}_s \quad [8]$$

where the vector \mathbf{r}_{qi} is the position of the spacecraft with respect to the central body, “ q ”, and the vectors \mathbf{f}_g and \mathbf{f}_s represent the acceleration of the spacecraft due to gravitational forces and solar radiation pressure, respectively. Both \mathbf{f}_g and \mathbf{f}_s are expressed here in terms of dimensional quantities, but are, in practice, nondimensionalized for use in numerical integration and differential corrections algorithms.

The terms on the right side of Eqn. [8] represent the components of the vehicle acceleration that are modeled to be consistent with the dynamics in the problem. The gravitational acceleration is governed by the familiar N -body relative equations,

$$\mathbf{f}_g = -\frac{\tilde{G}(m_i + m_q)\mathbf{r}_{qi}}{r_{qi}^3} + \tilde{G} \sum_{\substack{j=1 \\ j \neq i, q}}^n m_j \left(\frac{\mathbf{r}_{ij}}{r_{ij}^3} - \frac{\mathbf{r}_{qj}}{r_{qj}^3} \right) \quad [9]$$

where the vector \mathbf{r}_{qj} represents the position of each perturbing body with respect to the central body. The relative locations of the celestial bodies are delivered directly from DE405 ephemeris data. The vector \mathbf{r}_{ij} then corresponds to the position of each perturbing body relative to the spacecraft, “ i ”. The terms \tilde{G} and m_k are the gravitational constant and the mass of body “ k ”, respectively, expressed in terms of dimensional units. The acceleration due to solar radiation pressure is modeled as

$$\mathbf{f}_s = \frac{kAS_0r_0^2}{cm} \frac{\mathbf{r}_{Si}}{r_{Si}^3} \quad [10]$$

where the vector \mathbf{r}_{Si} represents the position of the spacecraft relative to the Sun. The constant k is a material property based on the reflectivity/absorptivity of the spacecraft, A is the cross-sectional area of the spacecraft, and S_0 is the solar flux associated with the nominal Sun-Earth distance, $r_0 = 1$ AU. The constants c and m correspond to the speed of light and the mass of the spacecraft, respectively.^{14–16} These parameters are spacecraft-specific and, in this investigation, are selected to be consistent with the ARTEMIS P2 spacecraft to improve the fidelity of the z -amplitude evolution analysis.

IV. NUMERICAL SCHEMES

To investigate the sensitivity of the z -amplitude evolution to various dynamical perturbations and to examine the placement of deterministic maneuvers to compensate for unfavorable z -amplitude histories, a reference solution is required. Unfortunately, the numerical computation of a continuous, end-to-end reference trajectory incorporating multiple revolutions of a Lissajous trajectory is nontrivial given that most

collinear libration point orbits are unstable and any simulation departs the orbit after 1-2 revolutions if not maintained. Numerical determination of a continuous, multi-revolution reference solution is possible, however, by employing a multiple shooting differential corrections algorithm. This reference is then incorporated into both the z -amplitude sensitivity analysis and in the deterministic correction maneuver placement strategy.

IV.I Multiple Shooting

The general multiple shooting approach is represented in the schematic in Fig. 4. An initial guess is discretized into n “patch points” connected by $n - 1$ trajectory arcs as illustrated in Fig. 4(a). Each patch point is represented by a six-dimensional vector, \mathbf{x}_i , and the integration time associated with each arc is T_i . Differential corrections in time-dependent ephemeris models also require the epoch at each patch point, denoted τ_i . The shortened notation \mathbf{x}_i^t , identifies the ter-

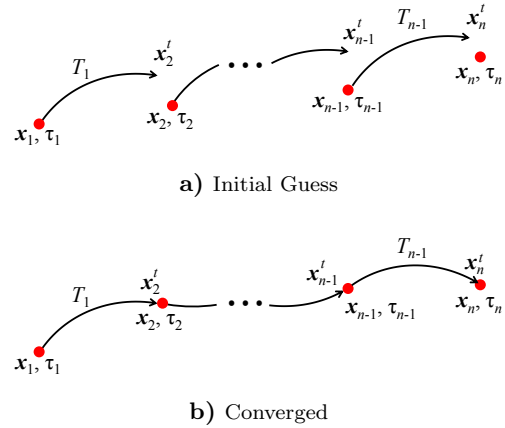


Fig. 4: Multiple Shooting Schematic

minal integrated state along each trajectory segment, $\mathbf{x}_i^t(\mathbf{x}_{i-1}, T_{i-1}, \tau_{i-1})$. In this application, Newton’s method is incorporated in the differential corrections process and converges to a solution that is continuous in position and velocity at all internal patch points and satisfies any additional problem-dependent end constraints.¹²

IV.II Designing a Reference Solution

Computing a reference solution is a critical first step to explore the sensitivity of z -amplitude evolution in quasi-periodic orbits and, ultimately, to determine the most effective placement of deterministic corrections maneuvers for meeting a set of end-of-mission requirements. Note that, in this investigation, “reference solution” is distinguished from “baseline.” Here, a baseline trajectory is a nominal path computed during the mission design phase. However, the term reference solution is used more broadly to denote a continuous, “end-to-end” trajectory that serves as an initial guess for a numerical corrections algorithm. During nominal mission operations, the baseline may be employed

as a reference solution but if the spacecraft deviates significantly from the original design, continually updating the reference is more effective. While reference solution design is largely application-dependent, it is summarized in three general steps:

- 1) Initial guess generation
- 2) Convergence in lower-fidelity model
- 3) Convergence in higher-fidelity model

In the case of libration point trajectories such as those for ARTEMIS, it is useful to complete steps 1) and 2) within the context of the circular restricted three-body problem and exploit well-established analysis tools for periodic orbits and invariant manifolds. For example, initial guesses for ARTEMIS-like trajectories are generated using stacked revolutions of planar Lyapunov orbits and arc segments along stable and unstable invariant manifolds as discussed by Pavlak and Howell.¹⁷ Multiple shooting is used to converge to a reference solution in the circular restricted three-body problem that can, in turn, be transitioned to any desired higher-fidelity dynamical models.

IV.III Out-of-Plane Amplitude Correction Strategy

Quasi-periodic orbits in the Earth-Moon system are highly sensitive and even small errors in position and/or velocity strongly influence the z -amplitude evolution downstream along the trajectory. For spacecraft such as ARTEMIS, with a relatively strict set of end-of-mission objectives, significant changes in z -amplitude can result in lunar arrival inclinations, for example, that are unacceptably large and do not satisfy mission requirements. There are a variety of potential approaches for correcting an undesirable z -amplitude evolution, but, for this initial investigation, a straightforward, systematic strategy is implemented.

A schematic for a deterministic ΔV placement strategy to rectify an unfavorable out-of-plane amplitude evolution appears in Fig. 5. The process begins with a continuous reference solution as in Fig. 5(a). Possible maneuver locations, i.e., patch points, appear in red and the green “X” denotes the desired end-of-mission requirement. The search for a low-cost maneuver to produce a favorable z -amplitude evolution commences by introducing a ΔV at each patch point – employing multiple shooting with any remaining segments along the reference solution as an initial guess. The process results in an entire set of trajectories, each with a ΔV in a different location; each arc satisfies the end-point constraints. The potential deterministic maneuvers along a sample reference path appear in Fig. 5(b). Each of these maneuvers represents one ΔV in a corrected trajectory that satisfies the desired set of end constraints though the individual resulting paths are not pictured. Note that, in general, a corrections scheme may not be successful in delivering

one ΔV from an arbitrary point on the path that satisfies the end-point constraints. Thus, a single ΔV that yields the desired end conditions may not exist for every patch point along a reference trajectory. The final step in the out-of-plane amplitude correction strategy is to select a single ΔV – typically the maneuver with the lowest magnitude – from the set of all possible maneuvers. In the schematic, ΔV_2 in Fig. 5(b) has the smallest magnitude and is applied in Fig. 5(c) as a deterministic maneuver along the reference trajectory that is plotted in black. The continuous, post-maneuver trajectory that satisfies the set of end-of-mission requirements is depicted in blue. It

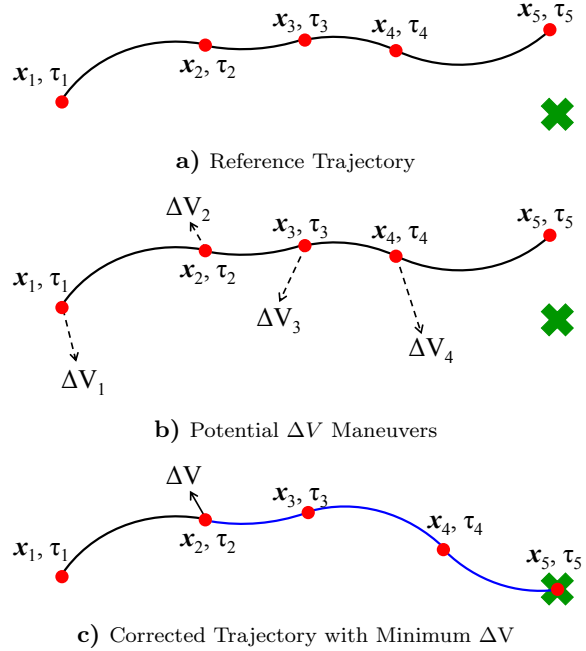


Fig. 5: Deterministic ΔV Placement Schematic

is important to note that future iterations of this algorithm could incorporate a strategy to optimize both the location and magnitude of the maneuvers. The current procedure, however, demonstrates the benefits of employing a reference solution and supplies a reliable and straightforward approach for correcting unfavorable out-of-plane amplitude evolution in a quasi-periodic libration point orbit using a single deterministic ΔV maneuver.

V. ARTEMIS P2 APPLICATION

An important scientific goal for the ARTEMIS mission is the collection of two-point measurements of the Earth’s magnetotail and the solar wind over a wide range of locations in the Sun-Earth and Earth-Moon regimes.⁸ In the final phase of the mission, the two ARTEMIS spacecraft enter lunar orbit to record a large number of “lunar wake crossings” in which the Moon is directly between the spacecraft and the Sun. To produce the desired sequence of wake crossings, it is critical that both probes achieve a near-planar

lunar orbit insertion at a specific Julian date as dictated by scientific requirements. In the highly sensitive Earth-Moon system, however, small perturbations are capable of altering the z -amplitude evolution of quasi-periodic orbits such as those employed by the ARTEMIS spacecraft in such a way that lunar arrival requirements are not satisfied. In fact, during mission operations for the P2 spacecraft, small errors in the L_2 injection state did result in an unfavorable out-of-plane evolution for the subsequent L_1 Lissajous orbit. A deterministic ΔV maneuver to correct the evolving z -amplitude had to be incorporated. Thus, the P2 trajectory is employed in this analysis to examine the effect of perturbations on z -amplitude evolution in quasi-periodic orbits and to demonstrate the application of a deterministic maneuver placement strategy.

V.I Reference Trajectory

A continuous, “end-to-end” reference trajectory representing the ARTEMIS P2 spacecraft is required for the z -amplitude sensitivity analysis and also serves as an integral part of the deterministic correction maneuver placement strategy. The P2 reference solution is designed consistent with the mission requirements described in Section II.II. Recall that this baseline path only incorporates the Earth-Moon libration point phase of the ARTEMIS P2 spacecraft and, thus begins at the L_2 orbit insertion. The trajectory is initially computed in the circular restricted three-body problem to exploit the wealth of dynamical systems theory knowledge in this regime. The entire process is detailed by Pavlak and Howell,¹⁷ but is summarized here. The initial guess for the reference is comprised of four distinct phases:

- 1) Unstable L_2 Lyapunov manifold arc
- 2) Stable L_1 Lyapunov manifold arc
- 3) 10 “stacked” revolutions of L_1 Lyapunov orbit
- 4) Unstable L_1 Lyapunov manifold arc

These individual segments are discretized into patch points and the multiple shooting algorithm returns a continuous reference solution in the CR3BP. During this process, the initial position is constrained to be the fixed value obtained from orbit determination data on October 3, 2010. If required, the CR3BP trajectory is transitioned to be continuous in an ephemeris model that might serve as a higher-fidelity reference, e.g., the ARTEMIS P2 baseline trajectory as displayed previously in Fig. 3. The trajectories employed throughout this analysis are computed using the parameters from Table 1. Numerical integration and differential corrections processes are conducted using quantities that are nondimensionalized by the characteristic values of length and time, denoted as l^* and t^* , respectively. The radius of the Moon is r_M , the gravitational parameters of the various bodies are represented by μ_k ,

| Parameter | Value | Units |
|-----------|---------------------|---------------------------------|
| l^* | 385,692.50 | km |
| t^* | 377,084.152667038 | s |
| μ_M | 398,600.432896939 | km ³ /s ² |
| μ_E | 4902.80058214776 | km ³ /s ² |
| μ_S | 132,712,440,017.987 | km ³ /s ² |
| r_M | 1738.2 | km |
| k | 1.17 | |
| A | 1 | m ² |
| m | 85.3527 | kg |
| S_0 | 1358.098 | W/m ² |
| r_0 | 149,597,927 | km |
| c | 299,792.458 | km/s |

Table 1: Problem Constants

and the remaining parameters as defined in Section III.II.

V.II Out-of-Plane Amplitude Sensitivity

The ARTEMIS P2 spacecraft emerged from the Earth-to-Moon transfer and entered the vicinity of the L_2 libration point on a trajectory with an unfavorable out-of-plane amplitude evolution prior to lunar orbit. A principal goal of this investigation is to examine if this phenomenon is the result of specific dynamical perturbations – namely, lunar eccentricity, solar gravity, and/or solar radiation pressure – or a product of the fundamental Earth-Moon multi-body gravitational environment. To explore the z -amplitude, let the baseline CR3BP ARTEMIS P2 solution in the lunar region serve as the “reference trajectory.” Then, a second path, termed the “perturbed reference trajectory”, is generated with an initial velocity that is altered from that of the reference to produce an unfavorable z -amplitude evolution. These two trajectories and their associated z -amplitude histories appear in Fig. 6.

The sensitivity of the out-of-plane evolution to various perturbing effects is evaluated by using the shooting algorithm to numerically produce continuous solutions in dynamical models of increasing fidelity and comparing the resulting z -amplitude profiles. The reference and perturbed reference trajectories in the CR3BP are employed as the initial guesses for the multiple shooting scheme. The four dynamical models include:

- 1) CR3BP
- 2) Moon-Earth Point Mass
- 3) Moon-Earth-Sun Point Mass
- 4) Moon-Earth-Sun Point Mass with SRP

Employing the circular restricted-three body solutions as initial guesses, the shooting algorithms use the reference and perturbed trajectories to converge in the three higher-fidelity ephemeris models. For each orbit, the initial position is always fixed and the epoch

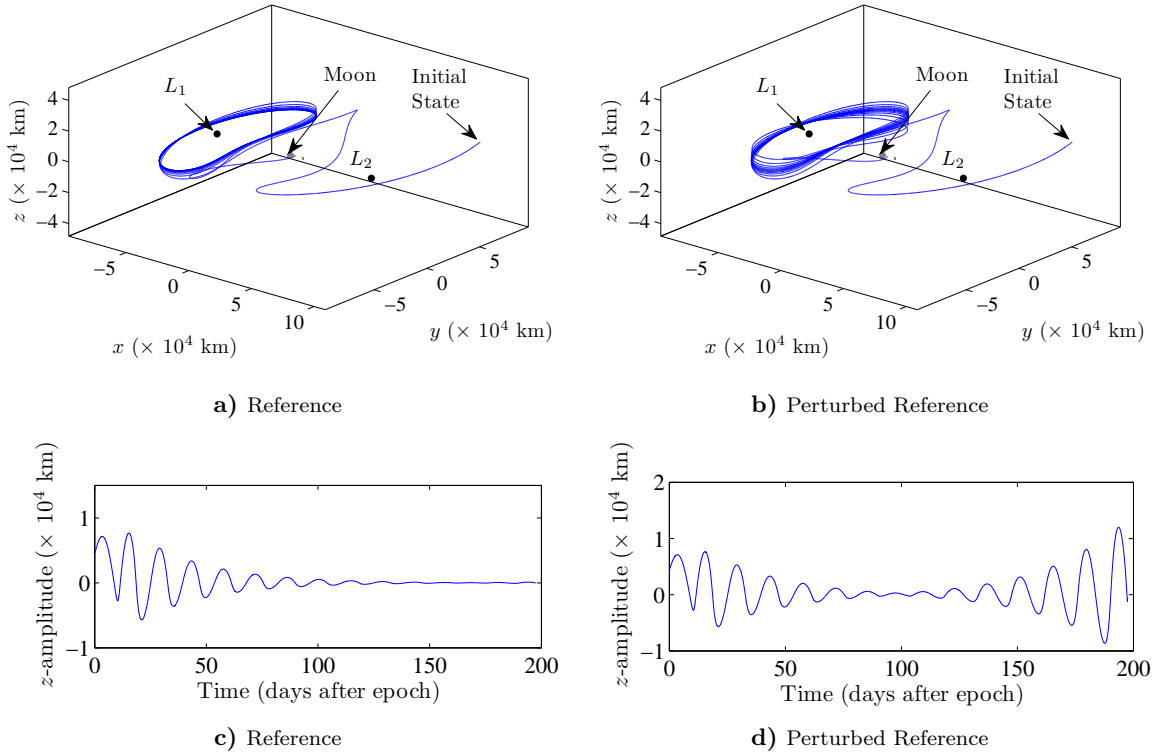


Fig. 6: The z -Amplitude Evolution for Two CR3BP Trajectories

and periapsis radius are constrained at lunar arrival. Note, however, that no constraint is placed on final inclination.

For both the reference and perturbed trajectories, the four converged paths lie relatively close together, thus, it is more useful to plot the difference in z -amplitude over time. Using the CR3BP solution as baselines, the resulting Δz -amplitude histories for the reference and perturbed trajectories constructed in higher-fidelity models appear in Fig. 7. The blue line denotes the difference in out-of-plane amplitude as determined between the circular restricted three-body problem and an Earth-Moon point mass ephemeris model; thus, the blue curve illustrates the impact of lunar eccentricity on z -amplitude. In comparison, the red line represents the variation between the CR3BP and an Earth-Moon-Sun point mass model. The line associated with the addition of solar radiation pressure to the model is not visible in this figure due to the fact that it is so close to the red curve, indicating that SRP has relatively little effect on the z -amplitude evolution of the ARTEMIS P2 spacecraft trajectory. This point is further illustrated by comparing the difference in out-of-plane amplitude produced in the Earth-Moon-Sun model and the Earth-Moon-Sun model incorporating SRP, respectively, as apparent in Fig. 8. The z -amplitude is altered by less than 5 km due to SRP for both the reference and perturbed trajectories. The exact cause of the unfavorable out-of-plane amplitude evolution that is experienced by the ARTEMIS P2 trajectory is difficult to determine definitively given

the chaotic nature of the Earth-Moon system. Thus, it is possible that both the reference and perturbed CR3BP trajectories exhibit very similar z -amplitude behavior in various higher-fidelity models. This result indicates the likelihood that the z -amplitude evolution of the ARTEMIS P2 path is due, not to a specific dynamical perturbation, that is, lunar eccentricity, solar gravity, or solar radiation pressure, but to the fundamental sensitivity associated with unstable libration point orbits in the Earth-Moon-spacecraft three-body problem.

V.III Out-of-Plane Amplitude Correction Example

For future spacecraft to operate efficiently in quasi-periodic libration point orbits, the out-of-plane amplitude evolution must be controlled with minimal ΔV . Low-cost solutions are particularly important for spacecraft with limited propellant such as ARTEMIS. Here, an out-of-plane amplitude correction strategy, as presented in Section IV.III, is applied to the ARTEMIS P2 trajectory as an example.

The perturbed ARTEMIS P2 trajectory, i.e., the trajectory with an unfavorable z -amplitude evolution in a Moon-Earth-Sun ephemeris model with SRP, is computed as in Section V.II. Note that the initial position is constrained to be fixed at the spacecraft arrival value on October 3, 2010. The trajectory is plotted in Fig. 9(a) and potential maneuver locations – indicated in red – are then identified at various downstream locations along the continuous perturbed reference trajectory. Approximately 130 maneuver locations are intro-

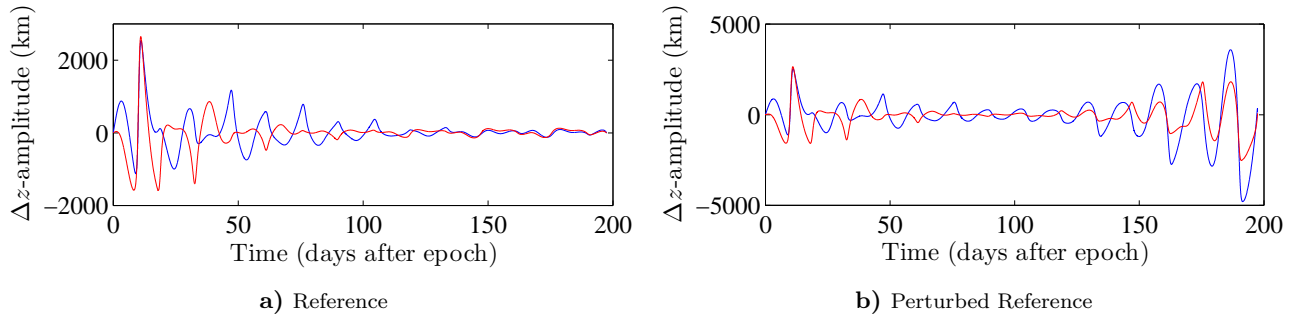


Fig. 7: Effect of Lunar Eccentricity (Blue) and Lunar Eccentricity + Solar Gravity (Red) on z -Amplitude

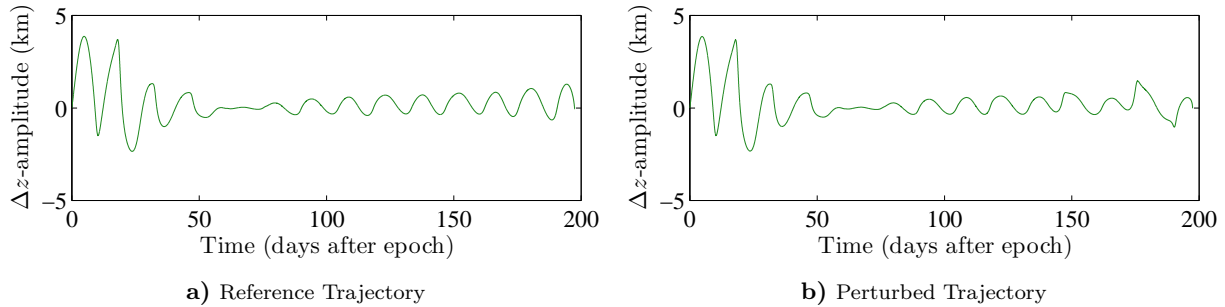


Fig. 8: Effect of SRP on z -Amplitude Evolution

duced in this example. Multiple shooting is employed to target from each potential maneuver location to a favorable, i.e., nearly planar, lunar arrival condition. Thus, ideally, the process yields 130 opportunities to meet the arrival constraints, with various ΔV levels, one for each ΔV option. However, the differential corrections algorithm rarely converges on a solution from *all* possible maneuver sites. A plot of the deterministic ΔV costs as a function of maneuver location appears in Fig. 9(b) and a zoomed view is displayed in Fig. 9(c). Each point represents a unique trajectory that satisfies the set of desired end constraints. Note that, as expected, it is generally less costly from a ΔV perspective to implement the z -amplitude correction maneuver early along the path. Also indicated in Fig. 9(b) and 9(c) are the two low-cost maneuver options computed in this simulation (red). The first maneuver – represented by the first red dot – is the least expensive of any maneuver computed along the perturbed reference trajectory and occurs just 1.8 days after L_2 insertion at a cost of 13.5 cm/s. The corrected trajectory appears in Fig. 10(a) and the corresponding z -amplitude evolution profile is displayed in Fig. 10(b). The red and blue lines represent the pre- and post-deterministic maneuver sections along the paths, respectively.

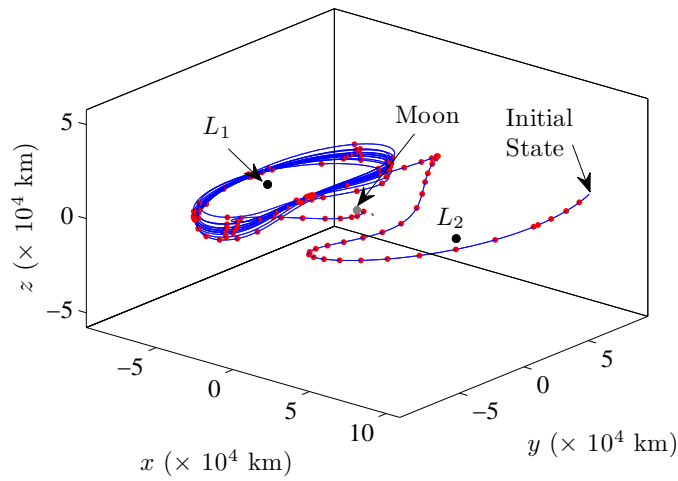
While it is most cost-effective to implement a ΔV as early as possible, it may be operationally undesirable or infeasible to plan and execute a deterministic correction maneuver only 1.8 days after L_2 insertion. However, a relatively low-cost maneuver to correct the out-of-plane amplitude evolution may still be possible during the L_1 Lissajous phase of the ARTEMIS

P2 trajectory. The second sample deterministic ΔV possesses a magnitude of 28.9 cm/s and occurs during the first revolution of the L_1 Lissajous orbit, 27.5 days after the L_2 insertion. The location and resulting corrected z -amplitude evolution for this second maneuver option are indicated in Fig. 11. In this initial investigation, while some low-cost options exist near the xy -plane, it is typically less expensive to introduce deterministic maneuvers at locations of maximum y -excursion which also correspond to regions of maximum out-of-plane amplitude for the ARTEMIS P2 trajectory. However, it is difficult to draw definitive conclusions from these unoptimized preliminary results. It is also important to note that optimization techniques could be used in future iterations of this out-of-plane amplitude corrections strategy to more efficiently design the deterministic corrections maneuvers.

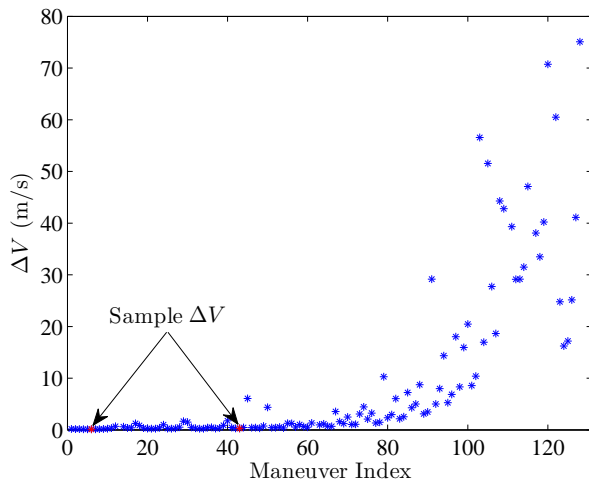
VI. CONCLUSIONS

As the first mission to exploit Earth-Moon libration point orbits, ARTEMIS spacecraft trajectories offer a number of challenges including the control of the z -amplitude evolution along a quasi-periodic orbit. Future missions in this regime will likely be required to address the same issues. This preliminary analysis employs the ARTEMIS P2 trajectory to consider the sensitivity of the out-of-plane evolution to various dynamical perturbations in the Earth-Moon system; a proposed orbit maintenance strategy to compute deterministic ΔV maneuvers that correct the unfavorable z -amplitude profiles is introduced.

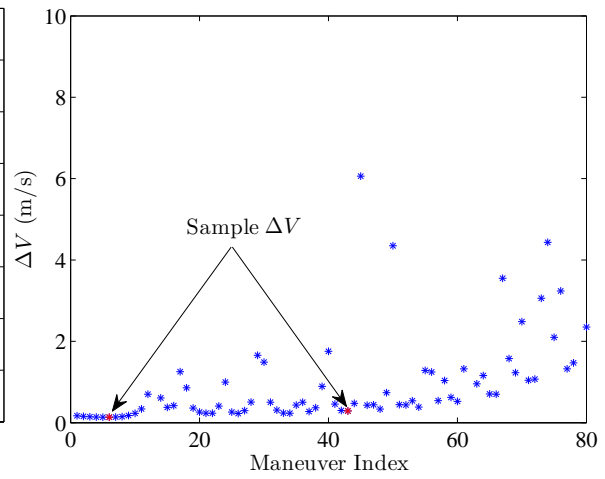
The source of an unfavorable z -amplitude evolution



a) Possible Maneuvers Along Reference Trajectory

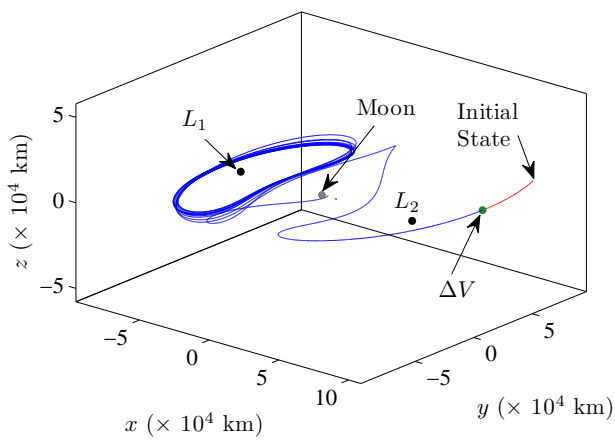


b) ΔV Cost vs. Maneuver Index

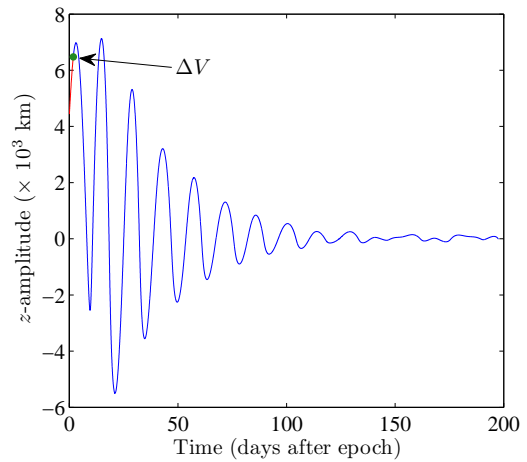


c) ΔV Cost vs. Maneuver Index (Zoomed)

Fig. 9: ΔV Cost at Various Maneuver Locations



a) Corrected Trajectory



b) Corrected z -Amplitude Profile

Fig. 10: Deterministic ΔV 1.8 Days After L_2 Insertion

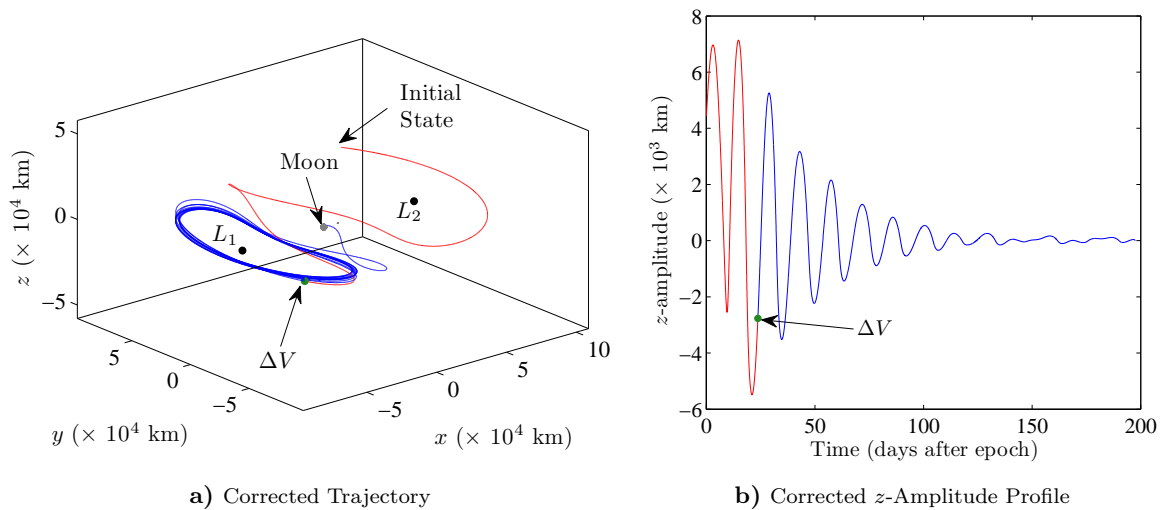


Fig. 11: Deterministic ΔV 27.5 Days After L_2 Insertion

is not attributed to a single dynamical contribution. It is demonstrated that favorable and unfavorable out-of-plane evolution histories are observable in dynamical models of varying degrees of fidelity. Perturbations such as lunar eccentricity, solar gravity, and solar radiation pressure are not the sole cause of unfavorable oscillations in z -amplitude such as those observed during operations of the ARTEMIS P2 spacecraft. A successful set of maneuvers for the P2 spacecraft did deliver the vehicle to the appropriate lunar orbit.¹¹ An alternative deterministic maneuver design approach is introduced, however, one that is reliable and efficient as an option for future application.

The out-of-plane amplitude corrections strategy is successfully applied to the ARTEMIS P2 spacecraft trajectory as a global-type search for deterministic maneuvers along the trajectory. It is typically more efficient to implement correction maneuvers as early as possible, but relatively inexpensive solutions are also available at a variety of locations along the P2 path. In general, maneuvers are less costly when performed at locations of maximum y -excursion which also correspond to regions of maximum z -amplitude. This correction strategy is sufficiently general and also highlights the utility of a continuous reference solution in highly sensitive dynamical regimes such as the Earth-Moon system.

ACKNOWLEDGEMENTS

The authors wish to thank David Folta and Mark Woodard for their assistance with research efforts at Goddard Space Flight Center. Portions of this work were completed at NASA Goddard and at Purdue University under NASA/GSFC Grant No. NNX10AJ24G and were also supported by the NASA Space Technology Research Fellowship (NSTRF) under Grant No. NNX11AM85H.

REFERENCES

- ¹R. Farquhar, "The Flight of ISEE-3/ICE: Origins, Mission History, and a Legacy," *AIAA/AAS Astrodynamics Specialist Conference and Exhibit*, Boston, Massachusetts, August 10-12, 1998. Paper No. AIAA-1998-4464.
- ²H. Franz, P. Sharer, K. Ogilvie, and M. Desch, "WIND Nominal Mission Performance and Extended Mission Design," *AIAA/AAS Astrodynamics Specialist Conference and Exhibit*, Boston, Massachusetts, August 10-12, 1998. Paper No. AIAA-1998-4467.
- ³C. Roberts and R. Short, "Injection Contingency Recovery Strategies for Halo Orbit Transfer Trajectories," *AIAA/AAS Astrodynamics Conference*, San Diego, California, July 29-31, 1996. Paper No. AIAA-1996-3600.
- ⁴P. Sharer and T. Harrington, "Trajectory Optimization for the ACE Halo Orbit Mission," *AIAA/AAS Astrodynamics Conference*, San Diego, California, July 29-31, 1996. Paper No. AIAA-1996-3601.
- ⁵F. Markley, S. Andrews, J. O'Donnell, and D. Ward, "The Microwave Anisotropy Probe (MAP) Mission," *AIAA Guidance, Navigation, and Control Conference and Exhibit*, Monterey, California, August 5-8, 2002. Paper No. AIAA-2002-4578.
- ⁶M. Lo, B. Williams, W. Bollman, D. Han, Y. Hahn, J. Bell, E. Hirst, R. Corwin, P. Hong, K. Howell, B. Barden, and R. Wilson, "Genesis Mission Design," *AIAA/AAS Astrodynamics Specialist Conference and Exhibit*, Boston, Massachusetts, August 10-12, 1998. Paper No. AIAA-1998-4468.
- ⁷M. Woodard, D. Folta, and D. Woodfork, "ARTEMIS: The First Mission to the Lunar Libration Points," *21st International Symposium on Space Flight Dynamics*, Toulouse, France, September 28-October 2, 2009.
- ⁸V. Angelopoulos, "The THEMIS Mission," *Space Science Reviews*, vol. 141, no. 1-4, pp. 5-34, 2008.
- ⁹NASA, *THEMIS Overview*, [Accessed August 31, 2011]. http://www.nasa.gov/mision_pages/themis/mission/index.html.
- ¹⁰D. Folta, T. Pavlak, K. Howell, M. Woodard, and D. Woodfork, "Stationkeeping of Lissajous Trajectories in the Earth-Moon System with Applications to ARTEMIS," *20th AAS/AIAA Space Flight Mechanics Meeting*, San Diego, California, February 14-17, 2010. Paper No. AAS 10-113.
- ¹¹D. Folta, M. Woodard, and D. Cosgrove, "Stationkeeping of the First Earth-Moon Libration Orbiters: The ARTEMIS Mission," *AAS/AIAA Astrodynamics Specialist Conference*, Girdwood, Alaska, July 31-August 4, 2011. Paper No. AAS 11-515.

¹²T. Pavlak, "Mission Design Applications in the Earth-Moon System: Transfer Trajectories and Stationkeeping," M.S. Thesis, Purdue University, West Lafayette, Indiana, 2010.

¹³B. Marchand, S. Scarritt, T. Pavlak, and K. Howell, "Investigation of Alternative Return Strategies for Orion Trans-Earth Injection Design Options," *20th AAS/AIAA Space Flight Mechanics Meeting*, San Diego, California, February 14-17, 2010. Paper No. AAS 10-128.

¹⁴R. Farquhar, "The Control and Use of Libration-Point Satellites," Tech. Rep., NASA Goddard Space Flight Center, NASA TR R-346, Greenbelt, Maryland, September, 1970.

¹⁵J. Bell, "The Impact of Solar Radiation Pressure on Sun-Earth L1 Libration Point Orbits," M.S. Thesis, Purdue University, West Lafayette, Indiana, 1991.

¹⁶M. Ozimek, "Low-Thrust Trajectory Design and Optimization of Lunar South Pole Coverage Missions," Ph.D. Thesis, Purdue University, West Lafayette, Indiana, 2010.

¹⁷T. Pavlak and K. Howell, "Strategy for Long-Term Libration Point Orbit Stationkeeping in the Earth-Moon System," *AAS/AIAA Astrodynamics Specialist Conference*, Girdwood, Alaska, July 31-August 4, 2011. Paper No. AAS 11-516.